CIMAC CONGRESS 19
VANCOUVER, JUNE 10–14, 2019

2019 | 179

Detailed Assessment of an Innovative Combined Gas-Diesel Injector for Diesel Ignited High-pressure Gas Direct Injection Combustion Concepts

10 - Latest Engine Component Developments - Fuel Injection & Gas Admission

Christoph Redtenbacher, LEC GmbH

Kevin Aßmus, LEC GmbH
Gottfried Lurf, LEC GmbH
Constantin Kiesling, LEC GmbH
Anton Tilz, Graz University of Technology
Andreas Nickl, Graz University of Technology

This paper has been presented and published at the 29th CIMAC World Congress 2019 in Vancouver, Canada. The CIMAC Congress is held every three years, each time in a different member country. The Congress program centres around the presentation of Technical Papers on engine research and development, application engineering on the original equipment side and engine operation and maintenance on the end-user side. The themes of the 2019 event included Digitalization & Connectivity for different applications, System Integration, Electrification & Hybridization, Emission Reduction Technologies, Low Carbon Combustion including Global Sulphur Cap 2020, Case Studies from Operators, Product Development of Gas and Diesel Engines, Components & Tribology, Turbochargers, Controls & Automation, Fuels & Lubricants as well as Basic Research & Advanced Engineering.

ABSTRACT

Diesel ignited high-pressure gas direct injection combustion concepts (gas-diesel combustion concepts) enable the use of gases with low methane numbers at a high compression ratio and consequently high thermal efficiency while keeping emissions of unburned hydrocarbons and thus methane very low. Woodward L'Orange GmbH has developed an advanced combined gas-diesel injector concept for high-speed applications of the gas-diesel combustion process. This paper assesses a prototype of this injector based on comprehensive investigations on an LEC injection rate analysis system and a high-speed single-cylinder research engine with a displacement of approximately 6 dm^3.

First, the challenges and requirements of fuel injection for gas-diesel engines are discussed and the investigated gas-diesel injector and the assessment methodology are introduced. Next, the injector is characterized based on the results of the measurements on the LEC injection rate analysis system. The total gas injection rate of all gas nozzle holes of the injector in relation to different operating parameters is analyzed as well as deviations in the injection characteristics of the individual nozzle holes and shot-to-shot fluctuations. Based on the results of the injector validation on the single-cylinder research engine, the benefits of exploiting the maximum permissible gas injection pressure of 500 bar are assessed and the use of hydrogen-enriched natural gas compared to natural gas is evaluated with regard to engine performance and emissions. Finally, the influence of the injector behavior on the engine results is discussed.

1 INTRODUCTION

Fully flexible dual fuel (DF) engines (cf. [14]) that are operated with either diesel or gaseous fuel as the main energy source have in common that operators benefit from the flexibility of adapting the fuel type to the market situation and redundancy in case the gas supply fails, cf. [2] [9] [18].

Diesel-gas engines, which are characterized by feeding of a premixed gas-air mixture into the engine and compression ignition of the cylinder charge via direct diesel injection into the combustion chamber, are known for their beneficial nitrogen oxide (NO_x) emission behavior; however, it remains a challenge to avoid methane (CH_4) slip and use gases with low methane numbers (MN) with this combustion concept, cf. [10] [15].

Gas-diesel engines (cf. [10]) operated according to the diesel cycle are a promising alternative. In DF operating mode, the gaseous fuel is directly injected into the combustion chamber at the end of the compression stroke. In addition, a small amount of diesel fuel is injected to initiate ignition of the inhomogeneous cylinder charge. Due to the resulting diffusion combustion, gas-diesel engines are not prone to knocking combustion, which allows the use of gases with low methane numbers at high compression ratios and therefore high thermal efficiency. With an appropriate combustion chamber geometry and injection strategy, the emission of unburned hydrocarbons (HC) and thus CH_4 can be kept very low, cf. [1]. Minimal CH_4 emissions are indispensable to exploiting the greenhouse gas saving potential of gaseous fuels with a low carbon to hydrogen ratio and thus comparatively lower CO_2 emissions than with conventional liquid fuels.

Adequate injection of the gaseous fuel and diesel into the combustion chamber of gas-diesel engines is key to meeting low emission targets with high engine efficiency. Advanced concepts use a combined gas-diesel injector with a coaxial arrangement of the gas nozzle and diesel nozzle in the center of the cylinder head, cf. [6]. However, the confined space within the cylinder head in high-speed large engines makes it a challenge to employ such a complex injector.

This paper assesses a prototype of a combined gas-diesel injector concept for high-speed applications of the gas-diesel combustion process that was recently developed by Woodward L'Orange GmbH. First, the paper discusses the challenges and requirements of fuel injection for gas-diesel engines and introduces the gas-diesel injector and the assessment methodology, which is based on comprehensive measurements on an LEC injection rate analysis system (LEC IRAS) and on a high-speed single-cylinder research engine (SCE) with a displacement of approximately 6 dm^3. Second, the paper characterizes the injector based on the results of the experimental investigations. It analyzes the total gas injection rate of all gas nozzle holes of the injector in relation to different operating parameters as well as hole-to-hole scattering effects and shot-to-shot variation effects. Furthermore, the benefits of exploiting the maximum permissible gas pressure of the injector are assessed and the use of natural gas (NG) enriched by hydrogen (H_2) is evaluated with regard to engine performance.

2 FUEL INJECTION FOR GAS-DIESEL ENGINES

2.1 Challenges and requirements

The challenge of fuel injection in gas-diesel engines is that both diesel and gas must be injected into the combustion chamber at a high pressure at the end of the compression phase. The system complexity resulting from having to provide two media is higher than with monofuel engine concepts. Tried and tested systems can be used for high-pressure generation, pressure control and media guidance, especially on the diesel side. However, the integration of two injection valves into the cylinder head poses a particular challenge. In slow-speed and medium-speed large engines with comparatively large cylinder bores, systems with two or even more fuel injectors may be feasible, cf. [2]. In high-speed large engines that feature high power density, however, the packaging of the components within the cylinder head is a critical issue because available space is limited. In addition, an optimal arrangement of the diesel and gas injection nozzles is important to ensure reproducible ignition of the inhomogeneous gas-air mixture by the self-ignited diesel fuel and a thermodynamically favorable combustion process in dual fuel operating mode. Furthermore, the targeting of the diesel sprays must fulfill the requirements for engine operation in diesel mode as well.

From investigations of diesel-gas engines with premixed combustion, for instance, it is well-known that a decentral position of the pilot diesel injector in the cylinder head has disadvantages compared to a central position of the pilot diesel injector, cf. [14]. The decentral ignition of the lean gas-air mixture results in asymmetrical flame propagation, which affects efficiency and combustion stability. Similar disadvantages can also be expected with the gas-diesel concept if the injectors are not arranged centrally.

Therefore, advanced injection systems use a combined gas-diesel injector with a coaxial

arrangement of the gas nozzle and the diesel nozzle, which is installed in the center of the cylinder head, cf. [6]. To obtain the best engine performance possible while complying with stringent emission legislation, the injector has to provide great flexibility in terms of injection timing, multiple injection and injection pressure with both gas and diesel injection. In addition, the diesel path of the injector has to cover a wide injection range from less than 10 % (dual fuel operation mode) to 100 % (diesel operation mode) energetic diesel fraction related to engine operation at nominal load. Despite the complexity of the combined injector, it must be competitive with multi-injector solutions in terms of injection reproducibility, service life and reliability.

2.2 Advanced combined high-pressure gas-diesel injector

Woodward L'Orange GmbH has recently developed an advanced combined high-pressure gas-diesel injector for large high-speed gas-diesel engines that meets the demanding requirements described in the previous section. By applying common rail technology, the diesel fuel and the gaseous fuel can be injected flexibly and independently of the other. The gaseous fuel is injected through three groups of gas nozzle holes; each group has a separate gas needle (one, two or three holes per group). All three groups are positioned symmetrically around the diesel nozzle 120° from each other, see Figure 1.

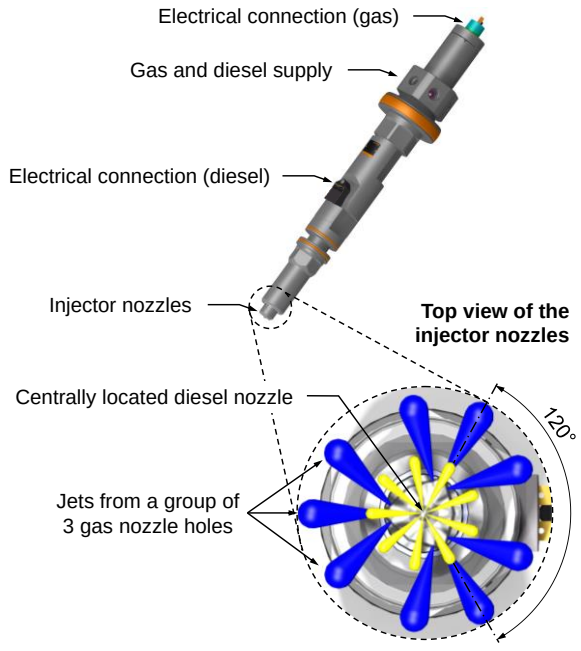

Figure 1: Combined high-pressure gas-diesel injector

Woodward L'Orange GmbH provided LEC GmbH with a prototype of this gas-diesel injector for a detailed investigation and evaluation of the injector concept. The maximum diesel rail pressure of this prototype is limited to 1600 bar in diesel operation mode. In dual fuel operation mode, the diesel rail pressure is limited to 1300 bar and the gas rail pressure is limited to 500 bar. The injector covers an operating range from around 1 % to 100 % energetic diesel fraction related to engine operation at nominal load. The gas nozzle and the diesel nozzle are equipped with nine nozzle holes each. Both gas injection and diesel injection are actuated by two independent valves which are electronically controlled by an engine control unit.

In addition to the main diesel fuel supply, this prototype injector requires two further diesel fuel supplies for the control oil and sealing oil systems, each of which has an independent pressure control. The control oil system supplies the switching force required to actuate the gas needles. The sealing oil system prevents gas leakage from each gas interface within the injector housing. Therefore, the sealing oil pressure has to be set slightly higher than the gas pressure. As a consequence, there is a slight leakage of sealing diesel oil into the gas path, which results in a small amount of diesel fuel being injected with the gaseous fuel through the gas nozzle. The two additional diesel fuel supplies will not be required in series applications of the gas-diesel injector since the control oil system and the sealing oil system will be provided within the injector with the required fuel pressures from the main diesel fuel supply.

3 METHODOLOGY

A twofold experimental approach was applied to assess the capabilities of the combined gas-diesel injector. First, the injector was thoroughly investigated on the LEC IRAS to determine the gas injection behavior of specific gas nozzle holes at varying boundary conditions. Since the gas-diesel injector uses nearly the same diesel injection technology as the well tested common rail diesel injector from the same manufacturer, the diesel injection behavior was not investigated in detail and will not be discussed in this paper. Second, SCE testing was carried out to validate the injector under operational conditions.

3.1 LEC IRAS

3.1.1 Measurement principle

The LEC IRAS makes use of the spray momentum measurement method. In this method, the axis of one specific spray hole of an injector nozzle is oriented perpendicular to a deflection plate that is placed in close proximity to the nozzle orifice. Assuming that the jet will be deflected radially from the spray axis when fuel is injected, a corresponding force (equivalent to the momentum

flux) can be recorded with a force sensor at the deflection plate in the direction of the jet axis, cf. [8] [5] [12]. The sampling rate of the force sensor must permit sufficient temporal resolution of a single injection event. In contrast to other experimental methods used to investigate the behavior of liquid fuel injectors such as the Bosch method [3] or the Zeuch method [19], the spray momentum measurement method has the advantage that the focus on one specific spray hole of a multi-hole nozzle allows the investigation of hole-to-hole variations, cf. [7]. Furthermore, this measurement method can be applied to liquid and gaseous fuel injectors and any burning gas can be used in the investigations if the test rig is equipped accordingly, cf. [5] [7].

The recorded momentum flux $\dot{I}$ is the basis for determining the gravimetric rate of injection designated as ROI according to equation (1). In this equation, m_{cycle} denotes the overall injected mass per single cycle and hole. m_{cycle} can be calculated from mass flow measurement during steady intermittent operation of the gas injector assuming an equal mass distribution from nozzle hole to nozzle hole and shot to shot. Cf. [7]

$$ROI = \sqrt{\dot{I}} * \frac{m_{cycle}}{\int \sqrt{\dot{I}}\, dt} \quad (1)$$

3.1.2 Test setup

The centerpiece of the LEC IRAS is the injection chamber with an inner volume of 1.3 dm³, see Figure 2.

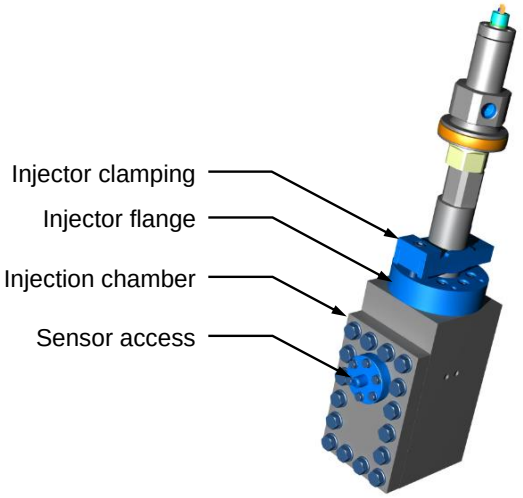

Figure 2: CAD mock-up of LEC IRAS

It is connected to an additional pressure accumulator with an inner volume of 4 dm³ (not illustrated). The injection chamber is limited to a maximum pressure of 175 bar and a maximum temperature of 70 °C. The gas-diesel injector is connected to the chamber by an injector flange and a clamping system. A lateral chamber opening provides access for a piezoelectric pressure transducer.

Before start of injector operation, an inert atmosphere and the desired back pressure are set in the chamber using a nitrogen supply system. The gas-diesel injector is supplied with up to 500 bar high-pressure gas by an ionic gas compressor and up to 2200 bar high-pressure diesel (required for control oil and seal oil) by a common rail pump. During steady intermittent injector operation, an adjustable pressure sustaining valve at the chamber outlet ensures constant pressure conditions in the chamber by continuously discharging gas from the chamber, cf. [7].

The continuous gaseous fuel mass flow to the injector is recorded with a Coriolis mass flow meter; the diesel mass flow is captured by a combined liquid fuel conditioning and consumption measurement device. The gas jet momentum flux is determined from the pressure signal, which is measured by the piezoelectric pressure transducer that has been fit into a sensor holder and whose membrane has been aligned perpendicular to the jet axis of the nozzle hole, and the membrane surface of the transducer, see Figure 3. The central nozzle hole of each gas nozzle hole group can be investigated with this experimental setup. In each test case, all nine gas nozzle holes are active during injector operation.

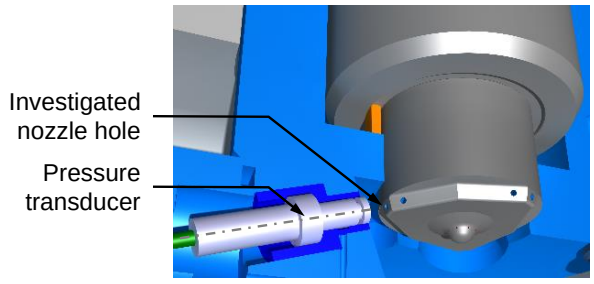

Figure 3: Cross section of the LEC IRAS

At each measurement point, the momentum flux traces of 60 consecutive injection events are recorded at a temporal resolution of 90 kHz.

3.1.3 Post processing

First, each measured momentum flux trace is smoothed. Based on the resulting curve, start of injection and end of injection are determined and a zero adjustment is carried out. The processed momentum flux signal is then used to calculate the ROI of the investigated nozzle hole according to equation (1). It is assumed that the measured total injected fuel mass (gaseous fuel mass plus diesel leakage mass) is evenly distributed among the nine gas nozzle holes, i.e. to calculate the ROI of one

specific nozzle hole, 1/9 of the total injected fuel mass is considered in the equation. In addition, an even distribution from shot to shot is assumed. For general analyses of injection behavior, the 60 calculated ROI cycles are averaged. For statistical evaluation of the shot-to-shot behavior, the ROI traces of the individual cycles are considered as well.

3.2 Single-cylinder research engine

All engine tests were carried out on a high-speed four-stroke single-cylinder research engine with the diesel-gas injector mounted in a central position in the cylinder head. The detailed engine specifications are given in Table 1.

Table 1: Technical specifications of the SCE

Rated speed	1500 rpm
Displacement	≈ 6 dm³
Compression ratio	16:1
Number of inlet/exhaust valves	2/2
Valve timing	Miller intake valve timing
Swirl/tumble	≈ 0/0
Charge air	Electrically driven air compressor with up to 10 bar boost pressure
Gas fuel supply	High-pressure ionic compressor with up to 600 bar gas pressure
Diesel fuel supply	Common rail system with up to 2200 bar diesel fuel pressure
Mass balances	Four balancing shafts to compensate for first and second-order inertia forces

The SCE features a single camshaft with Miller valve timing (cf. [13]) with intake valve closing before bottom dead center. The compression ratio was kept constant in all investigations. The engine is supplied with conditioned charge air, fuel, cooling water and lubricating oil to ensure reproducible testing conditions. The exhaust gas back pressure is controlled by a flap to simulate the presence of a turbocharger. A common rail system provides the diesel fuel for injection and the diesel fuel for the control oil system and the sealing oil system of the injector. Each of the diesel fuel supplies has a separate pressure control system. A high-pressure ionic compressor provides the required gas pressure. To investigate the use of H_2 enriched NG, a gas mixer provides the mixture of NG and H_2 at the requested methane number to the ionic compressor. The test bed is equipped with the latest crank angle and time-based measurement technology for all relevant parameters.

4 RESULTS

4.1 Characterization of the gas injection behavior

This section presents the results of the assessment of the nine-hole gas-diesel injector on the LEC IRAS. Each central gas nozzle hole of the three gas nozzle hole groups was thoroughly investigated. Three operating points representative of engine operation were selected from the extensive parameter variations performed (e.g., gas pressure, control oil pressure, sealing oil pressure, chamber pressure, duration of injection) for a detailed analysis of injector behavior.

With regard to the total fuel energy injected through the nine nozzle holes, one operating point at 400 bar gas rail pressure and one operating point at 500 bar gas rail pressure approximately correspond to the nominal engine load of 24 bar IMEP (100 % reference load). An additional operating point at 400 bar gas rail pressure corresponds to an engine load of 30 % (30 % reference load). When the investigations of the three central nozzle holes are compared, the total fuel energy introduced shows a deviation of less than ±0.1 % at 100 % reference load and ±5 % at 30 % reference load. Diesel pilot injection was not activated during the survey. The control oil and sealing oil pressures were adjusted to obtain optimal injector performance and minimal diesel leakage into the gas path. The boundary conditions of the investigations are summarized in Table 2.

Table 2: LEC IRAS boundary conditions

Reference engine speed	1500 rpm
Reference engine load	30 %/100 % of IMEP = 24 bar
Injected fuel	Natural gas
Gas rail pressure	400 bar/500 bar
Chamber pressure	130 bar

4.1.1 Total gas injection rate

The total gas injection rate (sum of the injection rates of all nine gas nozzle holes) has a decisive influence on the performance and emissions of the combustion process of the gas-diesel engine. Figure 4 shows the normalized total gas injection rates of the three operating points. These injection rates were determined by adding up the injection rates of all nine nozzle holes under the assumption that the injection rate of each of the three nozzle holes within a gas nozzle hole group is identical to the measured injection rate of the corresponding central gas nozzle hole. The normalized injection rate of each operating point is related to the corresponding total injected fuel mass. This fuel mass is the averaged value of the total injected fuel masses determined in the investigations of each of the three central nozzle holes. The figure also

presents the normalized total gas injection rates integrated via the crank angle. By definition, they always reach a value of 100 % at the end of injection. With regard to engine operation at a reference speed of 1500 rpm, the curves are plotted over an imaginary crank angle with a start of injector energizing at 0 °CA.

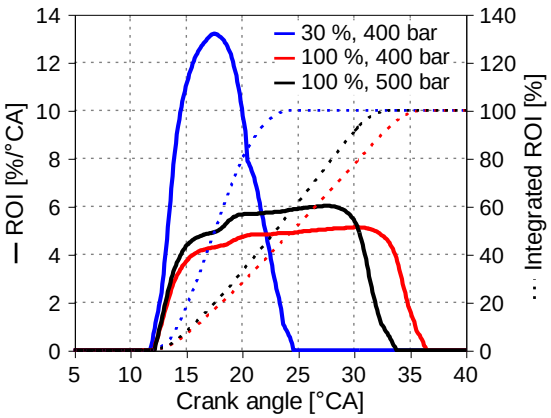

Figure 4: Normalized total gas injection rates and integrated normalized total gas injection rates

All operating points exhibit a similar hydraulic delay of about 12 °CA. By increasing the gas rail pressure from 400 bar to 500 bar at the reference load of 100 %, the injection duration is reduced by ≈ 3 °CA due to an increase in the normalized injection rate. The injection characteristics of both curves are similar with a distinct drop in the rising edge before the injection rate reaches a pronounced plateau. The injection rate at the reference load of 30 % has a relatively symmetrical curve, although two small kinks can be seen in the falling edge. No plateau is formed between the rising edge and the falling edge of the curve, which indicates ballistic operation of the injector at this operating point. As a result, the injection process is disproportionately longer than the operating point at 100 % reference load and 400 bar gas rail pressure. In the next step, the individual injection rates of the three central nozzle holes are analyzed in detail.

4.1.2 Hole-to-hole comparison

The three graphs in Figure 5 show the normalized injection rates and the corresponding integrated injection rates of the three central gas nozzle holes at the three operating points, which were discussed in the previous section. The normalized injection rates are related to 1/9 of the corresponding total injected fuel masses, which were measured separately for each nozzle hole and operating point.

Graphs a) and b) present the results at 100 % reference load and gas rail pressures of 500 bar and 400 bar, respectively. The injection rate characteristics are similar when the rail pressure influence at the same nozzle hole is compared. Furthermore, the injection rate characteristics of nozzle holes 2 and 3 are similar with a steep rising edge, a pronounced plateau during the phase when the gas needle is fully open and a falling edge with a slight kink. In contrast, the injection behavior of nozzle hole 1 deviates significantly. On the one hand, the injection rates of this nozzle hole show a very pronounced drop in the rising edge, which causes the drop in the rising edge of the total injection rates in Figure 4. On the other hand, injection duration is shorter due to a slightly longer hydraulic delay and earlier closing of the gas needle.

Graph c) depicts the results at 30 % reference load and a gas rail pressure of 400 bar. Similar to the operating points at 100 % reference load, the injection behavior of nozzle hole 1 deviates significantly from those of the other nozzle holes. Particularly striking are the closing time differences between the three gas needles of almost 5 °CA. These differences cause the two kinks observed in the falling edge of the corresponding total injection rate in Figure 4. Since there is no plateau in the injection rates, ballistic operation of all gas needles is assumed.

When interpreting the results, it should be noted that the masses injected through each of the nozzle holes at a single operating point are actually not the same. Since it is not possible to determine the exact masses with the applied approach, Figure 6 shows the post-processed and averaged momentum flux curves used to calculate the normalized injection rates in Figure 5. While the momentum flux curves of nozzle holes 2 and 3 are rather similar when compared at the same operating point, the curves determined at nozzle hole 1 are significantly less pronounced, especially at the operating point at 30 % reference load. Therefore, it is concluded that the actual fuel masses injected at nozzle hole 1 are lower than those at the other two nozzle holes. When interpreting the results in Figure 6, it should be remembered that the momentum flux is not directly proportional to the injection rate. Therefore, the differences in injected mass per crank angle are smaller than the differences in the momentum flux curves.

Due to the anomalous injection characteristic of nozzle hole 1, it is assumed that the gas jet pattern of the gas-diesel injector is irregular, independent of the operating point. From a thermodynamic perspective, a regular gas jet pattern is preferred; otherwise lower efficiencies and increased emissions from unburned fuel are expected similar to the irregular diesel spray pattern investigated in [11] and [16].

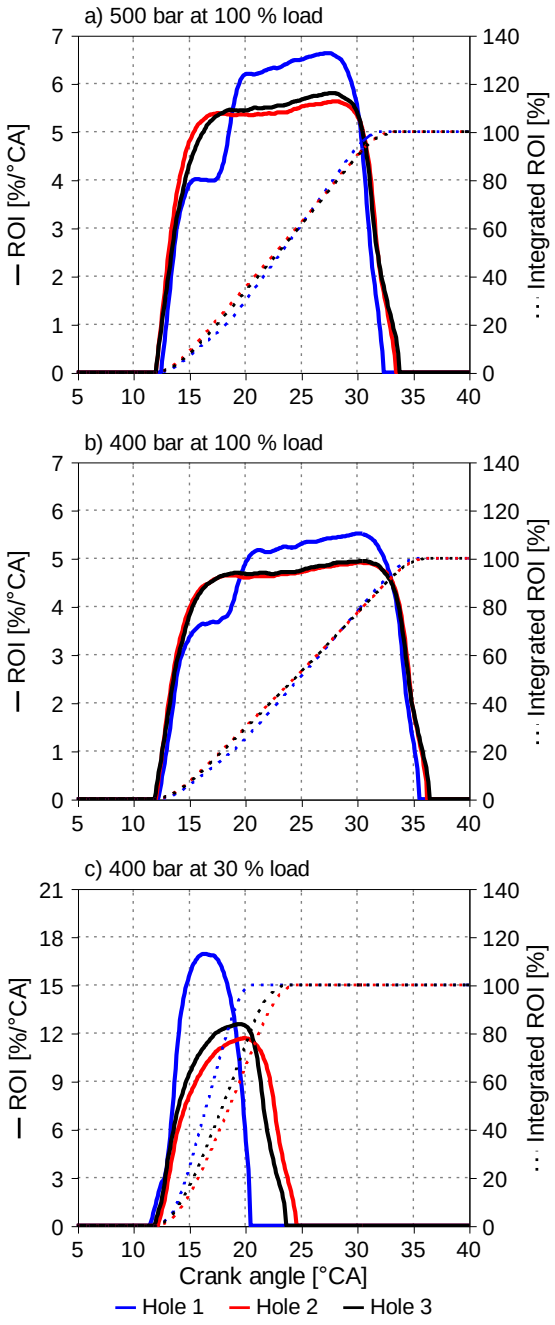

Figure 5: Normalized gas injection rates and integrated normalized gas injection rates of the central gas nozzle holes

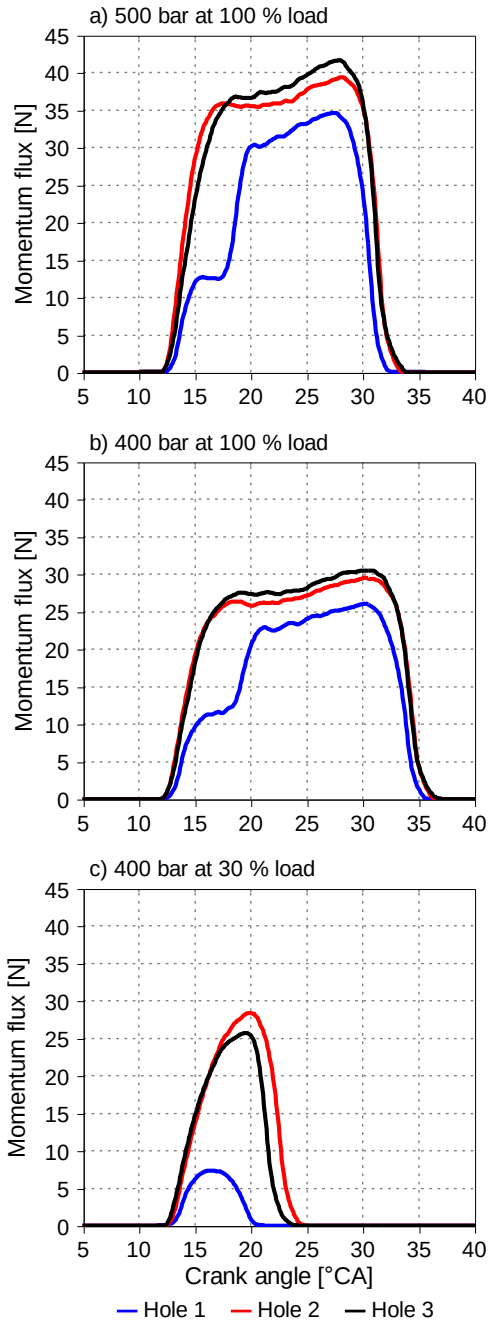

Figure 6: Momentum flux curves of the central gas nozzle holes

However, the extent to which the irregular injection behavior of this injector affects engine performance cannot be determined without comparative engine measurements that use an injector with a regular jet pattern. The cause of this irregular behavior is currently the subject of investigations at Woodward L'Orange GmbH.

4.1.3 Shot-to-shot comparison

The two operating points at 30 % and 100 % reference loads and 400 bar gas rail pressure were selected for analysis of the shot-to-shot fluctuations of the three central gas nozzle holes. Based on the 60 measured cycles per nozzle hole and operating point, Figure 7 presents the normalized averaged injection rates, which are identical to the corresponding curves in Figure 5, the normalized averaged injection rates ± standard deviation (SD) and the scatter range bordered by the envelopes.

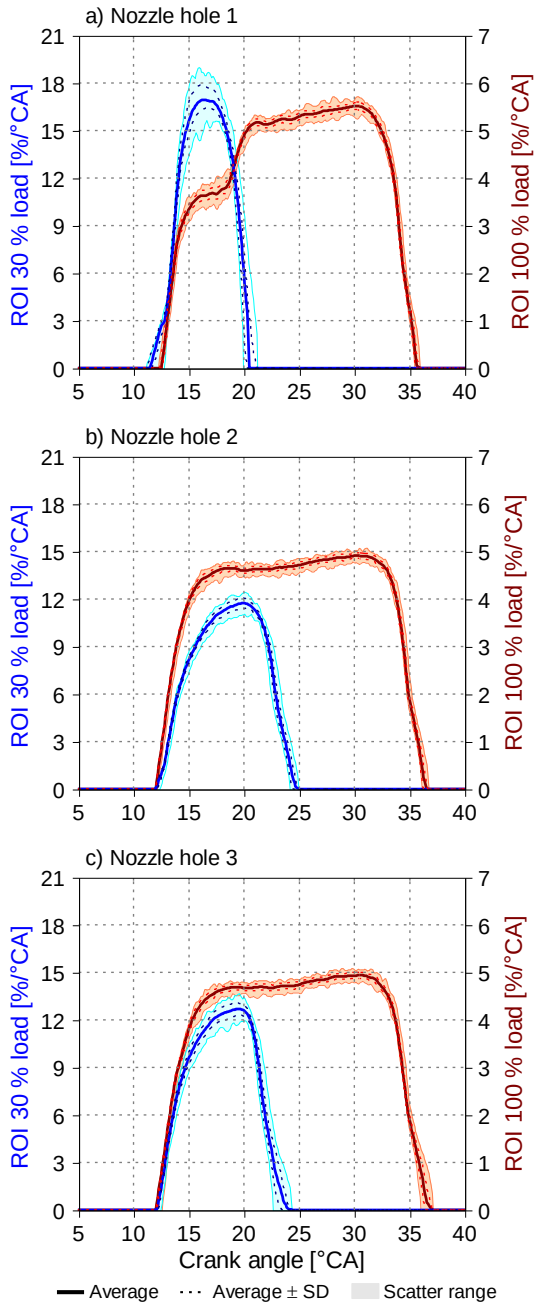

Figure 7: Shot-to-shot analysis at 30 % and 100 % reference loads and 400 bar gas rail pressure

The injection rate fluctuations of all nozzle holes at 30 % reference load are inherently greater than at 100 % reference load. Independent of the reference load, the start of injection of nozzle hole 1 fluctuates slightly while it is nearly stable at holes 2 and 3. In all cases, comparatively stable behavior during the early phase of gas needle opening is followed by an increased scatter range of the injection rates. Nozzle hole 1 in particular exhibits rather high fluctuations in the area of the distinct drop of the injection rate at 100 % reference load as well as in the transition area from needle opening to needle closing at 30 % reference load. With regard to the falling edge of the injection rates, the behavior of nozzle hole 3 is less stable than that of the other nozzle holes, resulting in a closing time scatter range of ≈ 1 °CA at 100 % reference load and ≈ 2 °CA at 30 % reference load. Overall, the shot-to-shot analysis reveals rather stable injection behavior with the gas-diesel injector emphasized by the small standard deviation range of the injection rates.

4.2 Validation of the injector on the SCE

Comprehensive parameter variations (e.g., timing of gas and diesel injections, pilot diesel fraction, excess air ratio (EAR), gas and diesel rail pressures, MN) were conducted on the SCE to validate the nine-hole gas-diesel injector under real engine conditions. This section presents selected results from an evaluation of engine performance and emission behavior at the maximum permissible gas rail pressure of 500 bar. The investigations were performed with two different gaseous fuel qualities, NG (MN 90) and H_2 enriched NG (MN 60). The latter was of particular interest since increased amounts of H_2 in the gas pipeline network are expected in power-to-gas scenarios, cf. [4] [17]. The investigated mixture of NG and H_2 demonstrates the capability of the gas-diesel combustion concept to exploit gaseous fuels with an energetic H_2 fraction of ≈ 15 %. Furthermore, the knock-resistant gas-diesel combustion concept is particularly suited to the use of these low-methane number gases. The boundary conditions applied to the measurement results discussed below are shown in Table 3.

Table 3: SCE boundary conditions

Engine speed	1500 rpm
IMEP	24 bar
Excess air ratio	2.1
Manifold air temperature	45 °C
Pilot diesel fraction	5 %
Diesel rail pressure	1300 bar
Gas rail pressure	500 bar / 400 bar
Methane number	NG: 90 / H_2 enriched NG: 60

Figure 8 shows the results of three injection timing variations plotted over the start of injector energizing of the diesel path, which is referred to as injection timing. The offset of the diesel injection timing from the gas injection timing was kept constant for all measurements. Two variations made use of NG, one at 400 bar and one at 500 bar gas rail pressure. One variation exploited H_2 enriched NG at 500 gas rail pressure.

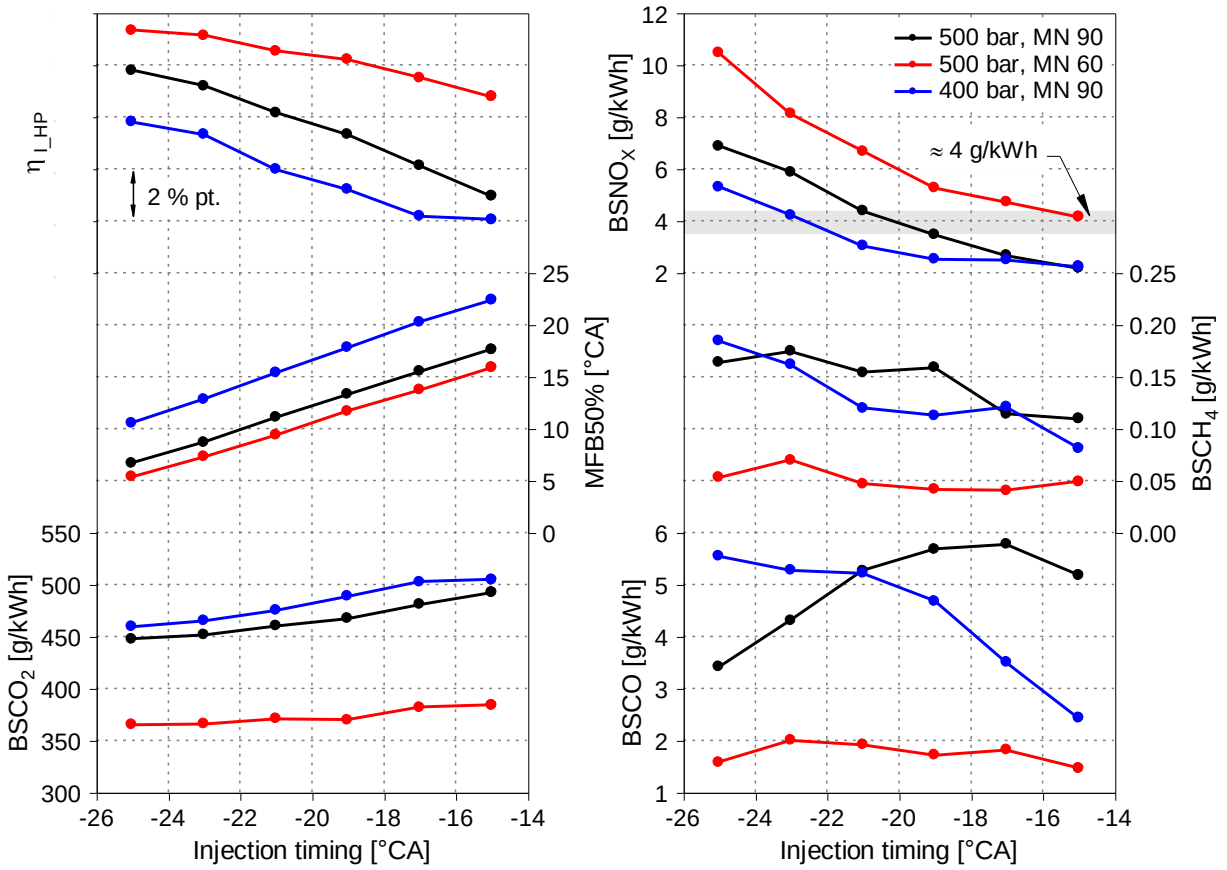

Figure 8: Influence of gas rail pressure and fuel quality on the gas-diesel combustion process

Increasing the gas rail pressure from 400 bar to 500 bar with NG at the same injection timing results in advanced combustion phasing and therefore higher indicated high-pressure efficiency (η_{I_HP}) but also higher brake specific NO_X emissions ($BSNO_X$). In the graph, the combustion phasing is represented by the crank angle at which 50 % of the total converted fuel energy has been converted (MFB50%). Because the friction mean effective pressure (FMEP) of the SCE is not representative, brake specific emissions are calculated based on the indicated specific emissions of the SCE and an estimated FMEP of a corresponding multicylinder engine. With regard to brake specific CH_4 emissions ($BSCH_4$) and brake specific CO emissions (BSCO), the pressure increase does not show a clear advantage. Depending on the injection timing, even higher emissions are observed, which may be caused by the increased injection pressure causing more gaseous fuel to reach the comparatively cold area close to the liner.

The fundamental advantage of the gas-diesel combustion process in that it can use gases with a low methane number was confirmed in the investigations with the H_2 enriched NG. As expected, no knocking occurred during all the measurements. When the two injection timing variations at 500 bar gas rail pressure are compared, the advantage of the gaseous fuel with MN 60 over that with MN 90 is considerable. The emissions of CO and CH_4 are significantly lower, which is most likely an effect of the reduced HC concentration in the low MN fuel. Furthermore, the ≈ 20 % reduction in brake specific CO_2 emissions ($BSCO_2$) is directly related to the reduced HC concentration in this fuel. Due to a fast combustion process, MFB50% is earlier with H_2 enriched NG than with NG at the same injection timing, which has a positive effect on efficiency and a negative effect on NO_x emissions.

To comprehensively evaluate the efficiencies of the three engine operating scenarios at similar NO_X emissions, a loss analysis according to Pischinger et al. [13] was performed for the measurement points at the $BSNO_x$ level of ≈ 4 g/kWh indicated by a grey bar in Figure 8. The results of this analysis are shown in Figure 9. The differences in η_{I_HP} arise from the differences in the efficiency of the ideal engine (η_{IE}) as well as the differences in losses from imperfect combustion ($\Delta\eta_{IC}$), real combustion ($\Delta\eta_{RC}$), and heat transfer ($\Delta\eta_{HT}$). η_{IE} is calculated based on a constant volume combustion process under consideration of the real charge. $\Delta\eta_{IC}$ are due to fuel species which leave the engine unburned or

partly burned. $\Delta\eta_{RC}$ are due to the deviation of the real combustion process from the constant volume combustion process of the ideal engine. $\Delta\eta_{HT}$ are due to heat transfer from the combustion gas to the combustion chamber walls.

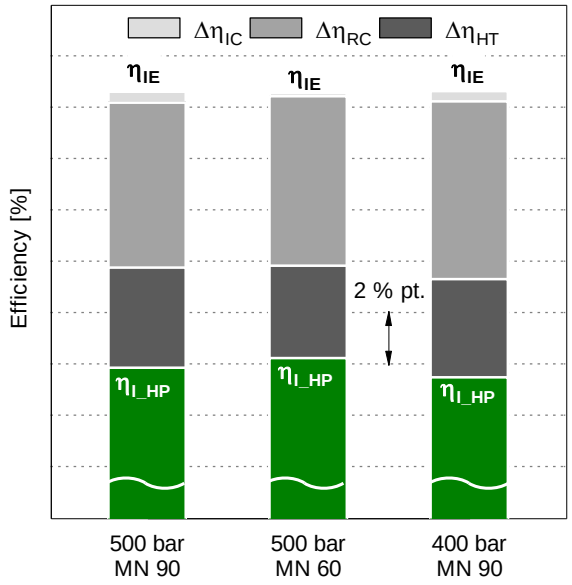

Figure 9: Loss analysis at $BSNO_X \approx 4$ g/kWh

The three operating scenarios start at a similar level of η_{IE} due to the constant EAR and compression ratio. In each case, diffusion combustion results in small losses from imperfect combustion. Due to the very low emissions of unburned and partly burned hydrocarbons, the losses are particularly small with H_2 enriched NG. Despite the comparatively late injection timing required to meet the $BSNO_x$ level of ≈ 4 g/kWh, losses from real combustion are only slightly higher with this fuel than with NG at 500 bar gas rail pressure. This is caused by the rather short and intensive heat release shown in Figure 10.

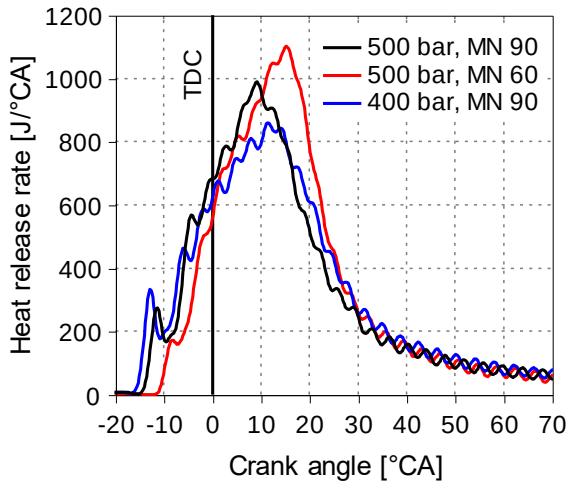

Figure 10: Heat release rates at $BSNO_X \approx 4$ g/kWh

The comparatively long combustion duration and delayed combustion with NG at 400 bar gas rail pressure lead to slightly higher losses from real combustion than at the other operating points. As a result of the late combustion start with H_2 enriched NG, the losses from heat transfer are smaller with this fuel than with NG. Overall, the smallest losses are obtained with H_2 enriched NG, which yields an advantage in η_{I_HP} of almost 0.5 % pt. compared to NG at 500 bar gas rail pressure. The scenario with NG at 400 bar gas rail pressure has the greatest losses and thus the lowest η_{I_HP}.

The gas-diesel injector performed reliably during all measurements. The combustion stability represented by the coefficient of variation of IMEP fell within a range of 1 % to 1.5 %, which indicates stable injector behavior. The diesel leakage from the sealing oil system into the gas path was determined to be ≈ 7 % at 400 bar gas rail pressure and ≈ 6 % at 500 bar gas rail pressure in relation to the total introduced fuel energy. This diesel admixing to the gas did not lead to conspicuous abnormalities in the combustion process. Despite the considerable amount of diesel in the gaseous fuel, ignition of the inhomogeneous fuel-air mixture was not possible without additional pilot diesel injection.

5 SUMMARY

The diesel ignited high-pressure gas direct injection combustion concept referred to as the gas-diesel combustion concept enables the use of gases with low methane numbers at high compression ratios and therefore high thermal efficiency while emissions of unburned HC und thus CH_4 are kept very low. Woodward L'Orange GmbH developed an advanced combined gas-diesel injector concept for high-speed applications of the gas-diesel combustion concept. This paper assessed a prototype of this injector based on comprehensive investigations on an LEC IRAS and on a high-speed SCE with a displacement of approximately 6 dm³.

An investigation was carried out on the LEC IRAS of the central gas nozzle holes of the three gas nozzle hole groups of the nine-hole gas-diesel injector. From the extensive parameter variations performed, three operating points representative of engine operation at 30 % of nominal engine load at 400 bar gas rail pressure and 100 % of nominal engine load at both 400 bar and 500 bar gas rail pressure were selected for a detailed analysis of injector behavior. The total gas injection rate of all gas nozzle holes indicates ballistic injector operation at 30 % reference load. At 100 % reference load, the injection rate curves reveal a distinctive drop in the rising edge before the injection rate reaches a pronounced plateau during the main injection phase.

In the next step, the individual injection rates of the three central nozzle holes were analyzed. While the injection behavior of two of the central gas nozzle holes is similar, the behavior of the third central gas nozzle hole exhibits significant deviations. At 100 % reference load, the injection rates of this nozzle hole exhibit a pronounced drop in the rising edge, which in turn causes the drop in the rising edge of the total injection rates. Furthermore, it is assumed that the fuel masses injected at nozzle hole 1 are smaller than those at the two other nozzle holes. Due to the different injection characteristics of the investigated nozzle holes, it is assumed that the gas jet pattern of the gas-diesel injector is irregular, independent of the operating point. The cause of this irregular behavior is currently the subject of investigations at Woodward L'Orange GmbH.

In addition, the shot-to-shot fluctuations of the gas nozzle holes were analyzed. Comparatively stable behavior during the early phase of gas needle opening is followed by an increased scatter range of the injection rates as injection continues. However, the shot-to-shot analysis revealed rather stable injection behavior of the gas-diesel injector overall.

Finally, extensive parameter variations were conducted on the SCE to validate the nine-hole gas-diesel injector under real engine conditions. The investigations were performed with two different gaseous fuel qualities, NG (MN 90) at 400 bar and 500 bar gas rail pressure and H_2 enriched NG (MN 60) at 500 bar gas rail pressure. Increasing the gas rail pressure from 400 bar to 500 bar provides advantages in indicated high pressure efficiency at $BSNO_x \approx 4$ g/kWh. When the influence of the fuel quality at 500 bar gas rail pressure is compared, the advantage of H_2 enriched NG over NG is considerable. The excellent opportunity to reduce greenhouse gases with the gas-diesel combustion concept is apparent from the considerable reduction in CH_4 and CO_2 emissions with H_2 enriched NG throughout the entire investigated operating range. In addition, there is a slight improvement in indicated high pressure efficiency at the $BSNO_x$ level of ≈ 4 g/kWh.

The gas-diesel injector performed reliably during all SCE measurements. The coefficient of variation of IMEP representative of combustion stability fell within a range between 1 % and 1.5 %, which indicates stable injector behavior.

6 ABBREVIATIONS AND ACRONYMS

$BSCH_4$	Brake Specific CH_4
BSCO	Brake Specific CO
$BSCO_2$	Brake Specific CO_2
$BSNO_x$	Brake Specific NO_x
CA	Crank Angle
CAD	Computer Aided Design
CH_4	Methane
CO	Carbon Monoxide
CO_2	Carbon Dioxide
DF	Dual Fuel
EAR	Excess Air Ratio
FMEP	Friction Mean Effective Pressure
H_2	Hydrogen
HC	Hydrocarbons
HRR	Heat Release Rate
$\dot{I}$	Momentum Flux
IMEP	Indicated Mean Effective Pressure
LEC IRAS	LEC Injection Rate Analysis System
m_{cycle}	Injected Mass per Cycle
MFB50%	50 % Mass Fraction Burned
MN	Methane Number
NG	Natural Gas
NO_x	Nitrogen Oxides
ROI	Rate of Injection
SD	Standard Deviation
SCE	Single Cylinder Research Engine
TDC	Top Dead Center
η_{IE}	Efficiency of the Ideal Engine
η_{I_HP}	Indicated High-Pressure Efficiency
$\Delta\eta_{IC}$	Losses from Imperfect Combustion
$\Delta\eta_{RC}$	Losses from Real Combustion
$\Delta\eta_{HT}$	Losses from Heat Transfer

7 ACKNOWLEDGEMENTS

The authors would like to acknowledge the financial support of the "COMET - Competence Centres for Excellent Technologies Programme" of the Austrian Federal Ministry for Transport, Innovation and Technology (BMVIT), the Austrian Federal Ministry of Science, Research and Economy (BMWFW) and the Provinces of Styria, Tyrol and Vienna for the K1-Centre LEC EvoLET. The COMET Programme is managed by the Austrian Research Promotion Agency (FFG).

8 REFERENCES AND BIBLIOGRAPHY

[1] Aßmus, K.; Redtenbacher, C.; Winter, H. et al.: "Simulation Based Predesign and Validation of a Diesel Ignited High-pressure Gas Direct Injection Combustion Concept", in: Leipertz, A. (ed.): "Engine Combustion and Alternative Concepts – ENCOM 2019" (= Berichte zur Energie- und Verfahrenstechnik (BEV), Vol. 19.1), Erlangen, 2019, pp. 83-94.

[2] Böckhoff, N.; Hanenkamp, A.: "Der 51/60DF von MAN Diesel SE – Der leistungsstärkste 4-Takt Dual Fuel Motor", in: Wissenschaftlich-Technisches Zentrum für Motoren- und Maschinenforschung Roßlau gGmbH (ed.): "Conference Proceedings, 5th Dessau Gas Engine Conference", Dessau, 2007, pp. 216-229.

[3] Bosch, W.: "Der Einspritzgesetzindikator, ein neues Meßgerät zur direkten Bestimmung des Einspritzgesetzes von Einzeleinspritzungen" in: "Motortechnische Zeitschrift", Vol. 25, Issue 7, 1964, pp. 268-282.

[4] Dörr, H.; Kröger, K.; Graf, F. et al.: "Untersuchungen zur Einspeisung von Wasserstoff in ein Erdgasnetz", in: "DVGW energie | wasser-praxis", Issue 11/2016, Bonn, 2016.

[5] Fimml, W.; Chmela, F.; Wimmer, A.: "Verfahren zur Messung der Einspritzrate unter motornahen Bedingungen", contribution at conference: "7. Tagung: Diesel- und Benzindirekteinspritzung", Berlin, 2010.

[6] Järf, C.; Sutkowski, M.: "The Wärtsilä 32GD engine for heavy gases", in: "Combustion Engines", Vol. 2, Issue 137, 2009, pp. 3-11.

[7] Kiesling, C.; Tilz, A.; Nickl, A. et al.: "Evaluation of Gas Injection Valves for Large Engines by Means of Spray Momentum Measurement", in: Tschöke, H.; Marohn, R. (ed.): "11. Tagung Einspritzung und Kraftstoffe 2018", Berlin, 2018, pp. 481-498.

[8] Luo, F.; Cui, H.; Dong, S.: "Transient measuring method for injection rate of each nozzle hole based on spray momentum flux", in: "Fuel", Vol. 125, 2014, pp. 20-29.

[9] Mohr, H.; Frobenius, M.: "Optimierung von Diesel-/Gas-Großmotoren für unterschiedlichste Anwendungen", in: Harndorf, H. (ed.): "Die Zukunft der Großmotoren III, 3. Rostocker Großmotorentagung", Rostock, 2014, pp. 138-149.

[10] Mooser, D.: "Brenngase und Gasmotoren", in: Mollenhauer, K.; Tschöke, H. (ed.): "Handbuch Dieselmotoren", 3rd edition, Berlin Heidelberg New York, 2007, pp. 132 ff.

[11] Napolitano, P.; Guido, C.; Beatrice, C. et al.: "Analysis of Nozzle Coking Impact on Emissions and Performance of a Euro5 Automotive Diesel Engine", in: "SAE International Journal of Engines", Vol. 6, Issue 3, Paper No. 2013-24-0127, 2013.

[12] Payri, R.; García, J. M.; Salvador, F. J. et al.: "Using spray momentum flux measurements to understand the influence of diesel nozzle geometry on spray characteristics", in: "Fuel", Vol. 84, Issue 5, 2005, pp. 551-561.

[13] Pischinger, R.; Klell, M.; Sams, T.: "Thermodynamik der Verbrennungskraftmaschine" (= technical book series: List, H. (ed.): "Der Fahrzeugantrieb"), 3rd edition, Vienna, 2009, pp. 338 ff, 349 ff.

[14] Redtenbacher, C.; Kiesling, C.; Wimmer, A. et al.: "Dual Fuel Brennverfahren – Ein zukunftsweisendes Konzept vom PKW- bis zum Großmotorenbereich?", in: Lenz, H. P. (ed.): "37th International Vienna Motor Symposium 28-29 April 2016. Volume 2: second day" (= Fortschritt-Berichte VDI Reihe 12, Nr. 799), Düsseldorf, 2016, pp. 403-428.

[15] Redtenbacher, C.; Malin, M.; Kiesling, C. et al.: "Gas and Dual Fuel Combustion Concepts: The Better Combustion Concepts for Large Engines?", in: "16. FAD-Konferenz. Herausforderung – Abgasnachbehandlung für Dieselmotoren. 7.11.-8.11.2018 in Dresden. Beiträge", Dresden, 2018, pp. 201-226.

[16] Som, S.; Ramirez, A. I.; Longman, D. E. et al.: "Effect of nozzle orifice geometry on spray, combustion, and emission characteristics under diesel engine conditions", in: "Fuel", Vol. 90, Issue 3, 2011, pp. 1267-1276.

[17] Sterner, M.; Stadler, I.: "Bedarf, Technologien, Integration", in: Sterner, M.; Stadler, I. (ed.): "Energiespeicher", 2nd edition, Berlin, 2017, pp. 468 ff.

[18] Watanabe, K.; Goto, S.; Hashimoto, T.: "Advanced development of medium speed gas engine targeting to marine and land", Paper No. 99, CIMAC Congress 2013, Shanghai.

[19] Zeuch, W.: "Neue Verfahren zur Messung des Einspritzgesetzes und der Regelmäßigkeit von Diesel-Einspritzpumpen", in: "Motortechnische Zeitschrift", Vol. 22, Issue 9, 1961, pp. 344-349.